Journal of Electron Spectroscopy and Related Phenomena 229 (2018) 42–46

Contents lists available at ScienceDirect

Journal of Electron Spectroscopy and Related Phenomena

journal homepage: www.elsevier.com/locate/elspec

The influence of shallow core levels on the shape of REELS spectra

M. Vos[a,*], P.L. Grande[b], G. Marmitt[b,1]

[a] Department of Electronic Materials Engineering, Research School of Physics and Engineering, The Australian National University, Canberra, Australia
[b] Instituto de Física, Universidade Federal do Rio Grande do Sul, Porto Alegre, RS, Brazil

ARTICLE INFO

Keywords:
Reflection electron energy loss spectroscopy
Dielectric function
Silicon

ABSTRACT

It is well established that the shape of spectra acquired using reflection electron energy loss spectroscopy (REELS) is determined by the dielectric function. Extracting the dielectric function from REELS spectra is a real challenge as it is governed by strong multiple scattering. It is generally assumed that the contribution of shallow core levels (with binding energies over 100 eV) to the REELS data can be neglected when one interprets valence band REELS data that usually extends to, at most, 100 eV energy loss. Here we show that, especially when incoming energies over 1 keV are used, this is not the case and that the intensity of the REELS spectrum can only be calculated correctly if the shallow core levels are taken into account. The implications for this for the extraction of the dielectric function from REELS data is discussed.

1. Introduction

It has been obvious for a long time that the shape of REELS spectra is determined by the dielectric function [1–3]. However extracting the dielectric function from a REELS spectrum is difficult, due to strong multiple scattering contributions, and the presence of surface and bulk losses. At higher energies the problem simplifies somewhat as the contribution of surface losses becomes small. There have been several attempts made to retrieve the dielectric function, in particular the Energy Loss Function in the optical limit (ELF), from REELS spectra, but the level of consistency obtained by different approaches is still somewhat disappointing and is thus difficult to assess the accuracy of the obtained results [4]. Most approaches aim to extract an ELF from one or more REELS spectra. Here we use the case of Si to calculate the REELS spectra based on previous estimates of the ELF in the optical limit.

In this paper we will show that it is not possible to obtain an accurate description of the first 100 eV of the REELS spectrum by considering only the first 100 eV of the ELF. It is demonstrated that, somewhat surprisingly, the ELF at larger energy losses has a significant impact on the intensity of the REELS spectrum in the low-loss region. This has significant implications for approaches that aim to derive the valence-band ELF from the low-loss REELS spectrum only [5–7] where one obtains an estimate of the loss function (either an effective loss function describing both surface and bulk excitations [7] or separately a bulk and surface loss function [5]) without considering the influence of semi-core electrons. It turns out that the presence of semi-core electrons affects the shape of the valence REELS spectrum significantly and hence their influence on the extracted loss function has to be investigated.

2. Experimental details

A silicon crystal was sputter-cleaned using 2 keV Ar^+ ions. No attempt was made to remove the lattice damage due to sputtering, and thus an amorphous layer will be present near the surface. Electrons with an incoming energy (E_0) of 40 keV were used. The incoming beam was directed along the surface normal and the analyser was at a backwards angle (scattering angle 135° with respect to the incoming beam). A concentration of Ar of several % can be present in the outer 50 Å layer [8] after sputter cleaning, but the depth probed by 40 keV is significant larger (200 Å for the elastic peak) ensuring that the effect of the Ar impurities is small. No asymmetry of the elastic peak due to Ar contribution (which mean recoil loss differs by 0.8eV from that of Si under these conditions) could be detected. The energy loss was determined over a relatively wide region (300 eV), by scanning the analyser energy. Multiple scans (≈20) were added. The incoming beam (≈10 nA) was measured by a current integrator producing a logical pulse for every pico-Coulomb of charge collected. The scan progresses to the next voltage after a pre-set number of pulses has been counted, ensuring equal exposure at all energy losses. The analyser was equipped with a two-dimensional detector, resolving the energy within an energy window and the direction of propagation of the outgoing electron [9]. It was checked that dead time effects were negligibly small. In spite of the

* Corresponding author.
E-mail address: maarten.vos@anu.edu.au (M. Vos).
[1] Present address: University Medical Center, Groningen, Netherlands.

https://doi.org/10.1016/j.elspec.2018.09.006
Received 10 July 2018; Received in revised form 4 September 2018; Accepted 19 September 2018
Available online 20 September 2018
0368-2048/

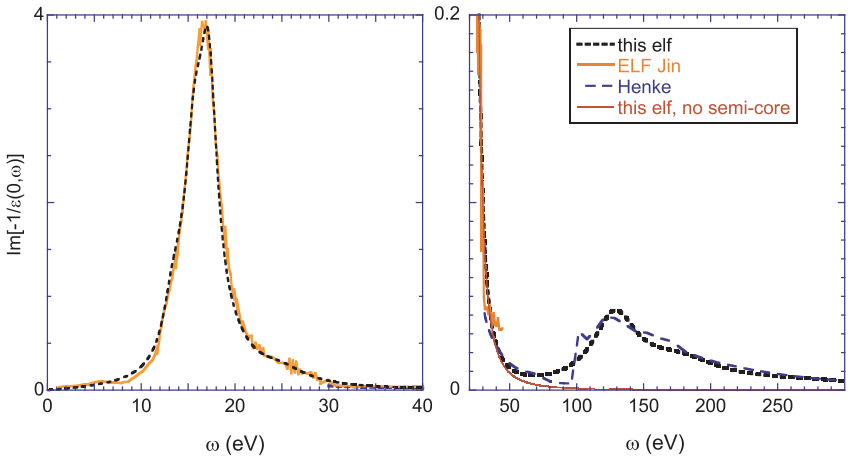

Fig. 1. The model energy loss function in the optical limit of Si used in this work. The valence band part was obtained by fitting the ELF published by Jin [10]. The deeper levels were introduced to get an approximate description of the loss function based on the atomic properties, as taken from Henke [11].

sputter-induced lattice damage there were still some effects of the lattice on the angular distribution of the outgoing electrons visible ('Kikuchi patterns') but by comparing the results of the detector for different angular ranges it was concluded that these did not affect the shape of the spectra in a major way.

3. Description of a REELS spectrum

For completeness we sketch here an outline of the framework that describes the trajectory of an energetic electron in matter. For more complete descriptions see e.g. [12–14].

Fast electrons impinging on matter interact both with the nuclei and target electrons. Due to the large difference in mass interaction with nuclei mainly deflects the electrons, but only a very small amount (up to a few eV for rare large-angle scattering events from light atoms) of energy is transferred (recoil effect). In electronic excitations ('inelastic scattering') the projectile energy is reduced, but for keV electrons the direction of propagation changes only by a small amount, as the momentum of electronic excitations, $\boldsymbol{q}$, is generally much less than that of the projectile. Thus, the trajectory of electrons inside matter is constructed by considering successive elastic and inelastic scatterings events, with some of the projectile's energy transferred at each interaction and its direction changed after an elastic collision.

The shape of the trajectory is due to the interaction of the projectile with (screened) nuclei. As significant deflections occur very close to the nuclei, the interactions of the electron with the nucleus can be taken to be the same for an atom in a solid and a free atom. The latter can be described well using partial wave analysis and this theory was used to calculate the differential elastic scattering cross section $\sigma_{el}(\theta)$ as implemented in the ELSEPA program [15].

After each integration step of the trajectory simulation, we also determine the probability that a certain number (N) of electronic excitations occurred. This is related to the inelastic mean free path (IMFP) λ. As the measured electrons have an energy that does not differ greatly from E_0 the same λ can be used for the whole trajectory. Then the probability of N inelastic events occurring along the step with length l is given by a Poisson distribution:

$$P_N(l) = \frac{e^{-l/\lambda}}{N!}\left(\frac{l}{\lambda}\right)^N. \tag{1}$$

The amount of energy loss in an inelastic event will differ from event to event and the probability distribution of a certain energy loss ω can be calculated from the dielectric function $\epsilon(q, \omega)$. It is proportional to the DIIMFP (differential inverse electron mean free path) $W_b(\omega)$:

$$W_b(\omega, E_0) = \frac{1}{\pi E_0}\int_{q_-}^{q_+}\frac{\mathrm{d}q}{q}\mathrm{Im}\left[\frac{-1}{\epsilon(q,\omega)}\right] \tag{2}$$

with $q_\pm = \sqrt{2E_0} \pm \sqrt{2(E_0-\omega)}$ the range of possible momenta of the inelastic excitation.(Here we use atomic units. For relativistic corrections at high energies see Ref. [16].) The $1/q$ term in the integral assures that small momentum transfers dominate the inelastic scattering, i.e. the assumption that inelastic scattering does not affect the direction of propagation of the projectile significantly is justifiable. If this distribution is normalised to unit area (the normalised differential inverse electron mean free path, NDIIMFP) then it gives the probability density that an energy ω is lost in an inelastic event. The required normalisation constant

$$C = \int_0^{E_0} W_b(\omega, E_0)d\omega \tag{3}$$

corresponds to the inverse of the inelastic mean free path: $C = 1/\lambda$.

For increase computational efficiency the procedure sketched above is implemented somewhat differently in PowerMeis [17,18] the Monte Carlo program which uses a variation of the connected trajectory formalism as described by Werner [19]. Two sets of trajectories are simulated: electrons starting from outside the sample propagating along the beam (incoming) and electrons moving from the detector towards the sample (outgoing). Time-reversal symmetry makes it possible to simulate the outgoing electrons in this way. Each trajectory is divided in many small segments Δl (with Δl much smaller than the elastic mean free path) and standard Monte Carlo procedures are used to simulate the deflections and energy loss (both due to recoil and inelastic excitations) along that segment. As a function of depth Z the energy loss and direction of propagation after each segment are tabulated. Finally, the two set of trajectories are combined at each depth z (weighted by $\sigma_{el}(\theta)$ with the angle θ determined by the difference in propagation direction of the incoming and outgoing electron) to form complete scattering events. This trajectory contributes to the REELS spectrum at the sum of the incoming and outgoing energy losses plus the recoil loss corresponding to a deflection over θ from the scattering nucleus.

In order to calculate the REELS spectrum we need thus an estimate of the dielectric function. For the case of silicon Jin et al derived an estimate of the energy loss function (ELF) $\mathrm{Im}[-1/\epsilon(0,\omega)]$ of Si from an extensive REELS study [10] and its main feature is a slightly asymmetric plasmon peak at $\omega = 17$ eV (Fig. 1, left panel). For ω values over ≈ 60 eV it is generally expected that the interaction of the target electrons with the projectile is not severely affected by solid state effects and one can use the atomic properties to calculate their contribution to $\epsilon(q, \omega)$ based on tabulations of Henke [11] (Fig. 1, right panel).

Table 1
The parameters to model the dielectric function of Si, as defined by Eq. (4). Oscillators in brackets correspond to the semi-core contributions.

i	A_i	Γ_i (eV)	ω_i (eV)
1	0.015	2	5.5
2	0.1	2.5	13.5
3	0.29	2.2	15.7
4	0.39	2.3	17.2
5	0.068	4	20
6	0.035	6	25
(7)	(0.011)	(40)	(130)
(8)	(0.006)	(80)	(180)
(9)	(0.002)	(150)	(280)

To get a description everywhere in (q, ω) space one often fits the ELF ($q = 0$) with a set of Drude-Lindhard oscillators with energy ω_i amplitude A_i and width Γ_i.

$$\mathrm{Im}\left[\frac{-1}{\epsilon(0,\omega)}\right] = \sum_i A_i \frac{\omega\Gamma_i\omega_i^2}{(\omega^2-\omega_i^2)^2+\omega^2\Gamma_i^2}. \quad (4)$$

Here we used Mermin oscillators, which coincide with the Drude-Lindhard oscillators at $q = 0$ but have dispersion 'built-in', but this does not affect the argument we want to make here. The fit is shown in Fig. 1 as well and actual parameters used are reproduced in Table 1. We can either fit only the valence loss function, or extend the fit to also model the semi-core related loss feature around $\omega = 120$ eV. In that case three more oscillators are used. Note that $\Sigma_i A_i = 0.944$ (0.925 without core level contributions) slightly less than 1, as this sum is related to the static refractive index n: $\Sigma_i A_i = 1 - (1/n)^2$ [20]. The corresponding DIIMFP is reproduced in Fig. 2 for three different energies E_0, covering the range of energies that are often used in REELS experiments.

As a cross check we can calculate the IMFP λ for our loss function and compare it with the estimate of the widely-used TPP-2M model [21]. This is done in Table 2. Especially for the dielectric function including the semi-core level the agreement with the TPP-2M model is very good, and without the semi-core level contribution the IMFP is slightly too large, indicating that the contribution of the semi-core levels to the IMFP is not negligible. At 300 eV the semi-core levels hardly affect the IMFP, at 4 keV it changes the IMFP at a 10% level, and at 40 keV its effect is about 15%.

To illustrate the influence of high energy losses on the REELS spectrum we now calculate the $N-$fold convolutions of the NDIIMFP,

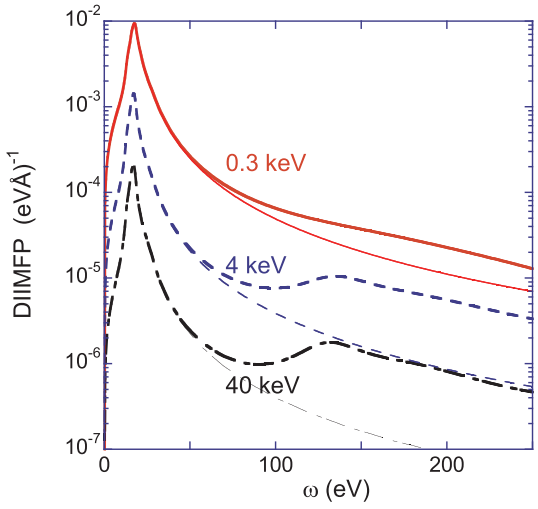

Fig. 2. The DIIMFP as calculated based on the model loss function (with core losses thick line, and without the core losses (thin lines)) for incoming electron energies of 0.3 keV, 4 keV and 40 keV. With increasing incoming energy the influence of the core losses on the DIIMFP become more pronounced.

Table 2
The inelastic mean free path based on the model ELF of Fig. 1 with, and without, the components related to the semi core levels as well as the values based on the (relativistic) TPP-2M approach. With increasing E_0 values the effect of the core levels increases, but it remains quite small (≈13%). Relativistic corrections were applied, as described in Ref. [16].

Energy keV	λ, no core (Å)	λ, incl core (Å)	λ TPP-2M (Å)
0.3	9.6	9.3	9.86
4	79.0	70.8	72.8
40	546	479	485

on which the REELS spectrum is based, with and without semi-core levels. By definition the NDIIMFP is normalised to 1. The area of the valence feature (maximum at $\omega = 17$ eV) of the NDIIMFP is 1 if the semi-core contributions are not included but varies from $A_v = 0.97$ (at 0.3 keV) to $A_v = 0.87$ (at 40 keV) if they are included. The energy distribution after N inelastic scattering events is given by the $N-$fold convolution of the NDIIMFP. After $N-$fold convolution the maximum is near $N \times 17$ eV and the area of the feature at this energy is A_v^N (with semi-core level included) or 1 (without semi-core level included). As is illustrated in Fig. 3 the effect of including the semi-core level changes the probability distribution greatly for large N values. This is understandable, as, for example for $N = 9$ the likelihood that any of the 9 excitations involves a semi-core electrons is considerable.

Generating a REELS spectrum using the Monte-Carlo method from the two dielectric functions produces strongly different outcomes, as shown in Fig. 4. The contribution of surface plasmons was neglected in this work, they affect the spectrum in a minor way for energy losses around 10 eV. Without the core level inclusion the generated intensity near 100 eV is much larger, and fails to mimic the experimentally obtained shape. With the core level included the agreement is much better. Then both experiment and simulation slowly decrease in intensity over the first 100 eV and levels out at larger energy losses, as for those energies trajectories with semi-core excitations contribute again.

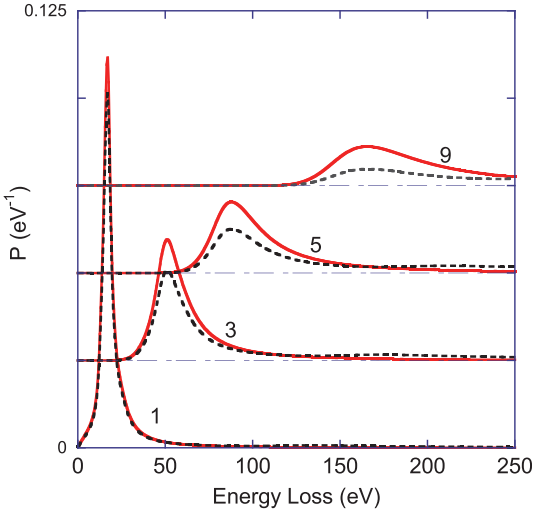

Fig. 3. The probability distribution of a specific energy loss after 1, 3, 5 and 9 energy loss events for the case of $E_0 = 40$ keV. (A vertical offset was applied for clarity). For 1 energy loss event this corresponds to the normalised DIIMFP. For N energy loss events the distribution is obtained by $N - 1$ times convoluting the normalised DIIMFP with itself. Distributions are given with (solid line) and without (dashed line) the core losses included. The influence of the core losses increases as N increases.

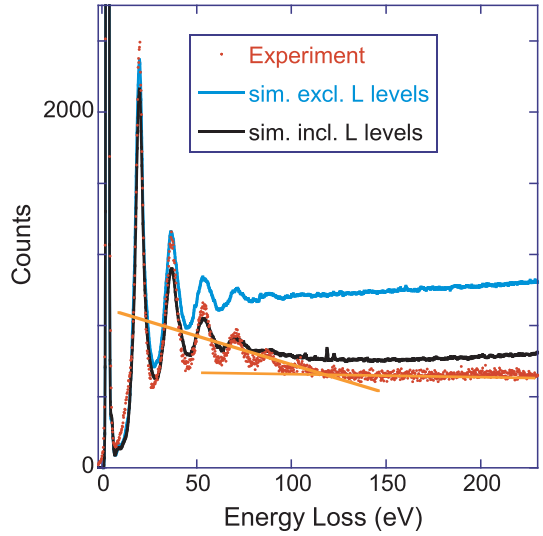

Fig. 4. Measured and simulated REELS spectrum for 40keV electrons impinging on Si. The simulations were done with (blue line) and without (black line) inclusion of the semi-core losses. Simulations and experiment are normalised to equal area of the elastic peak. For low losses the average intensity of the spectrum decreases with energy loss, but for losses larger than the semi-core levels the intensity is fairly constant, as indicated by the orange lines. (For interpretation of the references to color in this figure legend, the reader is referred to the web version of this article.)

4. Discussion and conclusion

We demonstrated that the semi-core levels of Si have a significant influence of the intensity of a REELS spectrum at energy losses lower than the semi-core binding energies. It is not possible to simulate the first 100 eV of the spectra well by considering valence ELF only. This implies that a determination of the valence-ELF based on the first 100 eV of the loss spectrum, without considering the semi-core levels, may introduce significant errors, especially for the ELF at larger energy losses. Similar results were obtained for the case of aluminum and should apply to a large number of elements that have shallow core levels. These effects are particularly pronounced at larger incoming energies used here (40 keV) but should also be significant in REELS experiments using energies of several keV or more.

If one uses an iterative scheme (assume a dielectric function, calculate a REELS spectrum, compare the outcome with experiment and adjust the dielectric function to improve agreement with experiment, see e.g. [22]) then the effects described here can be straightforwardly incorporated by calculating the DIIMFP over a larger energy loss range than the measured REELS spectrum. On the other hand, if one uses a deconvolution approach to derive either the NDIIMFP [19,23] or a weighted mixed surface-bulk effective cross section [6] directly from the experiment then the effect of the semi-core levels is harder to trace. Werner's approach [23] solves the multiple scattering problem in Fourier space, where convolutions simplify to multiplications. However, for the Fourier transform knowledge of the spectrum for all energy losses is required, hence this method does not necessarily circumvent the problem described here.

To investigate the influence of the semi-core electrons on the deconvolution method we used the simulated data obtained by the MC procedure, with and without core levels as if they are experimental data, and try to extract the single-loss distribution using the Tougaard-Chorkendorff procedure [6]. Briefly, if one normalises the spectrum such that the elastic peak has unit area, then one considers the intensity I_1 the first channel beyond the elastic peak due a single energy loss event of magnitude E_1, i.e. for this normalisation the probability for an energy loss event with magnitude E_1 is I_1. Let a_n be the number of

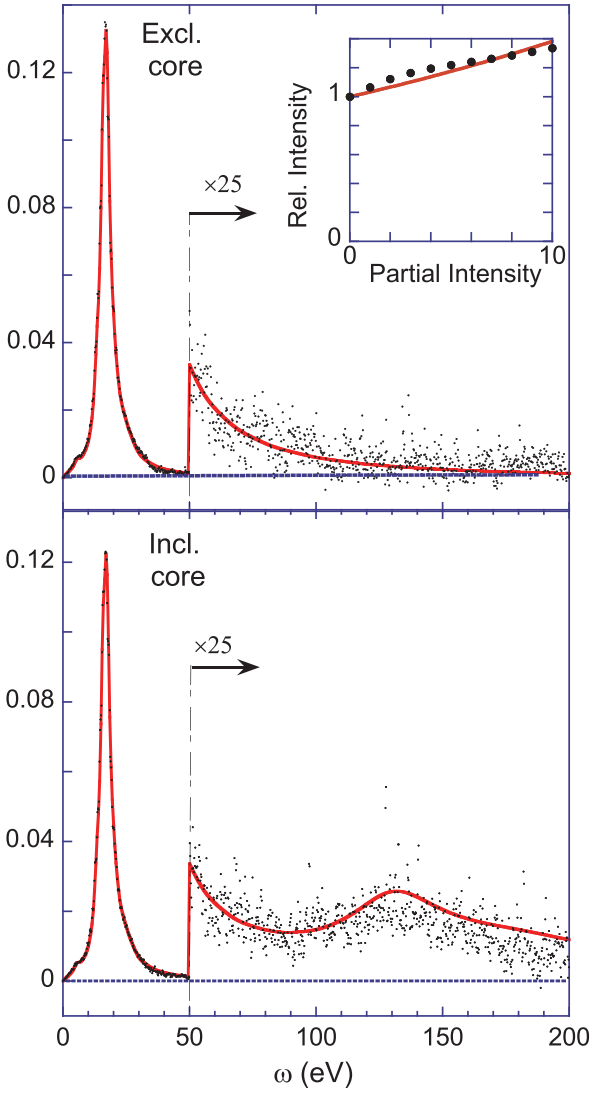

Fig. 5. The NDIIMFP as obtained from the results of the Monte Carlo simulations, without (top) and with (bottom) the semi-core contribution to the loss function, using the Tougaard-Chorkendorff deconvolution procedure (dots). The full line is the normalised NDIIMFP as calculated from the model dielectric function using Eq. (2) without (top) and with (bottom) the semicore electrons included. The insert shows the partial intensities as obtained from a separate Monte Carlo simulation (dots) and these partial intensities can be quite well fitted in the form of $a_n = c^n$ (line).

detected electrons that have experienced n inelastic events (the 'partial intensities'). For our elastic peak normalisation $a_0 = 1$. For this deconvolution procedure to be valid it is required that $a_n = a_1^n$ [24,25]. I_1 is a_1 times the NDIIMFP at E_1. Part of the intensity in the next channel I_2 is due to a single energy loss event with magnitude $2E_1$ but part of its intensity is due to trajectories with 2 inelastic events of magnitude E_1. The probability of this is I_1^2. Subtracting this amount from I_2 we obtain the probability for energy loss with magnitude E_2. In this way one can retrieve the a_1 times the NDIMFP up to energy E_x without knowledge of the spectrum for $E > E_x$.

The Monte Carlo procedure does not consider surface excitations, so in this case (in contrast to actual REELS data) the result of the deconvolution procedure should correspond simply to the NDIIMFP. In Fig. 5 we show the result of the deconvolution procedure for the MC data. Somewhat surprisingly, the height of the plasmon is almost the same in both deconvoluted spectra. Thus the considerable difference in shape of the 2 Monte Carlo generated spectra is corrected for by inferring in the deconvolution procedure a NDIIMFP with slightly different height of

the main loss feature. The deconvoluted results indeed follow closely the NDIIMFP as calculated via Eq. (2) with and without inclusion of the semi-core electrons. At larger losses the core level contribution, not obvious in the raw Monte Carlo result, can be distinguished but is heavily affected by noise.

A dielectric function was used based on Mermin oscillators which strictly applies to free-electron materials only. This approach has dispersion 'build-in' without adjustable parameters. It turns out (see Fig. 4) that this approach somewhat underestimates the height of the first two plasmons. Yubero et al. [26] used a Drude-Lindhard approach and adjusted the α parameter, describing the dispersion to 0.5 (smaller than the free-electron value) resulting in a better description of the spectra. The same dielectric function as in Ref. [26] was used by Pauly and Tougaard [27] without inclusion of the semi-core levels. They performed Monte Carlo simulations of REELS spectra describing the surface layer (thickness X_s) by an effective loss function and using for larger depth the bulk loss function. Surprisingly they found that the intensity of the REELS spectrum at larger energy losses ($\approx$100 eV, corresponding to depth much larger than X_s) depends strongly on the choice of X_s. Here we show that the intensity at larger losses (especially for larger incoming energies) is also strongly influenced by the semi-core levels and would influence the value of X_s for which the best agreement between experiment and simulation is obtained.

In conclusion a small contribution of the semi-core levels to the loss function can have a significant impact on the shape of a REELS spectrum and, when simulating a spectrum, has to be incorporated for a complete understanding of the experiment. Analysis based on the Tougaard-Chorkendorff deconvolution procedure avoids largely the complications due to the presence of the semi-core levels.

Acknowledgements

This work was realized with support from CNPq, Conselho Nacional de Desenvolvimento Científico e Tecnológico – Brazil and the the Australian Research Council.

References

[1] R.H. Ritchie, Plasma losses by fast electrons in thin films, Phys. Rev. 106 (1957) 874–881, https://doi.org/10.1103/PhysRev.106.874.
[2] D. Pines, Elementary Excitations in Solids, Benjamin, New York, 1963.
[3] C. Tung, Y. Chen, C. Kwei, T. Chou, Differential cross sections for plasmon excitations and reflected electron-energy-loss spectra, Phys. Rev. B 49 (1994) 16684–16693, https://doi.org/10.1103/PhysRevB.49.16684.
[4] M. Vos, P. Grande, The relation between the electron energy loss spectra of hafnia and its dielectric function, Surf. Sci. 630 (2014) 1–8, https://doi.org/10.1016/j.susc.2014.06.008.
[5] W. Werner, K. Glantschnig, C. Ambrosch-Draxl, Optical constants and inelastic electron-scattering data for 17 elemental metals, J. Phys. Chem. Ref. Data 38 (2009) 1013–1092, https://doi.org/10.1063/1.3243762.
[6] S. Tougaard, I. Chorkendorff, Differential inelastic electron scattering cross sections from experimental reflection electron-energy-loss spectra: application to background removal in electron spectroscopy, Phys. Rev. B 35 (1987) 6570–6577, https://doi.org/10.1103/PhysRevB.35.6570.
[7] F. Yubero, S. Tougaard, Model for quantitative analysis of reflection-electron-energy-loss spectra, Phys. Rev. B 46 (1992) 2486–2497, https://doi.org/10.1103/PhysRevB.46.2486.
[8] G. Sachse, W. Miller, C. Gross, An investigation of RF sputter etched silicon surfaces using helium ion backscatter, Solid-State Electron. 18 (5) (1975) 31, https://doi.org/10.1016/0038-1101(75)90045-3.
[9] M. Vos, G.P. Cornish, E. Weigold, A high-energy (e, 2e) spectrometer for the study of the spectral momentum density of materials, Rev. Sci. Instrum. 71 (2000) 3831–3840, https://doi.org/10.1063/1.1290507.
[10] H. Jin, H. Shinotsuka, H. Yoshikawa, H. Iwai, S. Tanuma, S. Tougaard, Measurement of optical constants of Si and SiO_2 from reflection electron energy loss spectra using factor analysis method, J. Appl. Phys. 107 (2010) 083709, https://doi.org/10.1063/1.3346345.
[11] B. Henke, E. Gullikson, J. Davis, X-ray interactions: photoabsorption, scattering, transmission, and reflection at e = 50-30,000 eV, $z = 1 - 92$, At. Data Nucl. Data Tables 54 (1993) 181, https://doi.org/10.1006/adnd.1993.1013.
[12] R. Shimizu, Z.-J. Ding, Monte Carlo Modelling of electron-solid interactions, Rep. Prog. Phys. 55 (1992) 487, https://doi.org/10.1088/0034-4885/55/4/002.
[13] W.S.M. Werner, Simulation of electron spectra for surface analysis using the partial-intensity approach (pia), Surf. Interface Anal. 37 (2005) 846–860.
[14] R.F. Egerton, Electron Energy-Loss Spectroscopy in the Electron Microscope, Plenum Press, New York, 1996.
[15] F. Salvat, A. Jablonski, C.J. Powell, ELSEPA Dirac partial-wave calculation of elastic scattering of electrons and positrons by atoms, positive ions and molecules, Comput. Phys. Commun. 165 (2005) 157–190, https://doi.org/10.1016/j.cpc.2004.09.006.
[16] H. Shinotsuka, B. Da, S. Tanuma, H. Yoshikawa, C.J. Powell, D.R. Penn, Calculations of electron inelastic mean free paths. XI. data for liquid water for energies from 50 eV to 30 keV, Surf. Interface Anal. 49 (2016) 238, https://doi.org/10.1002/sia.6123.
[17] G. Marmitt, Metal Oxides of Resistive Memories Investigated by Electron and Ion Backscattering (PhD Thesis Universidade Federal do Rio Grande do Sul), (2017) https://www.lume.ufrgs.br/bitstream/handle/10183/170451/001053460.pdf?sequence=1.
[18] http://tars.if.ufrgs.br/.
[19] W. Werner, Trajectory reversal approach for electron backscattering from solid surfaces, Phys. Rev. B 71 (2005), https://doi.org/10.1103/physrevb.71.115415.
[20] M. Vos, P. Grande, Simple model dielectric functions for insulators, J. Phys. Chem. Solids 104 (2017) 192, https://doi.org/10.1016/j.jpcs.2016.12.015.
[21] S. Tanuma, C.J. Powell, D.R. Penn, Calculations of electron inelastic mean free paths. V. Data for 14 organic compounds over the 50-2000 ev range, Surf. Interface Anal. 21 (1994) 165–176, https://doi.org/10.1002/sia.740210302.
[22] B. Da, Y. Sun, S.F. Mao, Z.M. Zhang, H. Jin, H. Yoshikawa, S. Tanuma, Z.J. Ding, A reverse Monte Carlo method for deriving optical constants of solids from reflection electron energy-loss spectroscopy spectra, J. Appl. Phys. 113 (2013) 214303, https://doi.org/10.1063/1.4809544.
[23] W. Werner, Differential surface and volume excitation probability of medium-energy electrons in solids, Phys. Rev. B 74 (2006) 075421, https://doi.org/10.1103/PhysRevB.74.075421.
[24] W.S. Werner, Differential probability for surface and volume electronic excitations in Fe, Pd and Pt, Surf. Sci. 588 (2005) 26, https://doi.org/10.1016/j.susc.2005.05.023.
[25] W. Werner, Simple algorithm for quantitative analysis of reflection electronenergy loss spectra (REELS), Surf. Sci. 604 (2010) 290–299, https://doi.org/10.1016/j.susc.2009.11.019.
[26] F. Yubero, S. Tougaard, E. Elizalde, J.M. Sanz, Dielectric loss function of Si and SiO2 from quantitative analysis of REELS spectra, Surf. Interface Anal. 20 (1993) 719, https://doi.org/10.1002/sia.740200817.
[27] N. Pauly, S. Tougaard, Model for Monte Carlo simulations of reflection electron energy loss spectra applied to silicon at energies between 300 and 2000 eV, Surf. Interface Anal. 42 (6-) (2010) 1100, https://doi.org/10.1002/sia.3277.